Exploring the sub-eV neutrino mass range with supernova neutrinos

Enrico Nardi
INFN, Laboratori Nazionali di Frascati, C.P. 13, I00044 Frascati, Italy
and Instituto de Física, Universidad de Antioquia, A.A. 1226, Medellín, Colombia

Jorge I. Zuluaga
Instituto de Física, Universidad de Antioquia, A.A. 1226, Medellín, Colombia
(Received 30 July 2003; revised manuscript received 27 January 2004; published 12 May 2004)

A new method to study the effects of neutrino masses on a supernova neutrino signal is proposed. The method relies exclusively on the analysis of the full statistics of neutrino events, it is independent of astrophysical assumptions, and does not require the observation of any additional phenomenon to trace possible delays in the neutrino arrival times. The sensitivity of the method to the sub-eV neutrino mass range, defined as the capability of disentangling at 95% C.L. the case $m_\nu = 1$ eV from $m_\nu = 0$, is tested by analyzing a set of synthetic neutrino samples modeled according to the signal that could be detected at SuperKamiokande. For a supernova at the Galactic center success is achieved in more than 50% of the cases. It is argued that a future Galactic supernova yielding several thousands of inverse β decays might provide enough information to explore a neutrino mass range somewhat below 1 eV.

DOI: 10.1103/PhysRevD.69.103002 PACS number(s): 96.40.Tv, 14.60.Pq, 97.60.Bw

During the past few years, the large amount of data collected by solar [1] and atmospheric [2] neutrino experiments provided strong evidence for nonvanishing neutrino masses. The recent KamLAND result [3] on the depletion of the neutrino flux from nuclear power plants in Japan gave a final confirmation of this picture. Since in the standard model (SM) of particle physics all neutrino species are massless, this constitutes the first direct evidence for new physics, and provides important information for developing theories beyond the SM. However, to date all the evidence for neutrino masses comes from oscillation experiments that are only sensitive to mass square differences and cannot give any information on single mass values. The importance of measuring the absolute value of neutrino masses cannot be understated. It is presently being addressed by means of a remarkably large number of different approaches, ranging from laboratory experiments to a plethora of methods that rely on cosmological considerations. Recent reviews can be found in [4]. From the study of the end point of the electron spectrum in tritium β decay, laboratory experiments have been able to set the limit $m_{\nu_e} < 2.2$ eV [5]. This is already close to the sensitivity limit of on-going experiments. If neutrinos are Majorana particles, the non-observation of neutrinoless double β decay can constrain a particular combination of the three neutrino masses. Interpretation of these experimental results is difficult due to large theoretical uncertainties related to nuclear matrix elements calculations. This is reflected in a model-dependent limit $m_\nu^{eff} < 0.35$–1.24 eV [4,6]. A tight bound $\Sigma_i m_{\nu_i} < 0.7$ eV was recently set by the Wilkinson Microwave Anisotropy Probe (WMAP) Collaboration [7] by combining measurements of cosmic microwave background anisotropies with data from bright galaxies redshift surveys [8] and other cosmological data. However, this limit becomes much looser if the set of assumptions on which it relies is relaxed (see [9] for discussions of this point). Therefore it is quite important to keep looking for alternative ways to measure the neutrino masses. Model independent limits can be more reliably established by combining complementary experimental information and, needless to say, it would be of utmost importance if the mass values could be measured by means of more than one independent method.

Already a long time ago it was realized that supernova (SN) neutrinos can provide valuable information on the neutrino masses [10]. The basic idea relies on the time-of-flight delay Δt that a neutrino of mass m_ν and energy E_ν traveling a distance L would suffer with respect to a massless particle:

$$\frac{\Delta t}{L} = \frac{1}{v} - 1 \approx \left(\frac{5.1\ \text{ms}}{10\ \text{kpc}}\right)\left(\frac{10\ \text{MeV}}{E_\nu}\right)^2\left(\frac{m_\nu}{1\ \text{eV}}\right)^2, \qquad (1)$$

where for ultra-relativistic neutrinos we have used $1/v = E_\nu/p_\nu \simeq 1 + m_\nu^2/2E_\nu^2$. The dispersion in the arrival time of about 20 electron anti-neutrinos from supernova SN1987A was used in the past to set the model independent limit $m_{\bar{\nu}_e} < 30$ eV [11]. This limit can become significantly tighter under some specific assumptions. For example a recent detailed reanalysis obtained, within the SN delayed explosion scenario, the limit $m_{\bar{\nu}_e} < 5.7$ eV [12].

Since SN 1987A, several efforts have been carried out to improve the sensitivity of the method, while waiting for the next explosion within our Galaxy. Often, these approaches rely on ''timing'' events related to the collapse of the star core, which are used as benchmarks for measuring the neutrino delays. The emission of gravitational waves [13,14], the ν_e neutronization burst [14], the initial steep raise of the neutrino luminosity [15], and the abrupt interruption of the neutrino signal due to a further collapse into a black hole [16] have been used to this aim. However, there are some drawbacks to these methods: firstly only neutrinos with arrival time close to the benchmarks are used, and they represent only a small fraction of the total; secondly the observa-

tion of the benchmark events is not always certain, and in any case some model dependence on the details of the SN explosion is generally introduced.

The method we want to propose is free from these drawbacks: it relies only on the measurement of the neutrino energies and arrival times, and it uses the full statistics of the detected signal, thus allowing us to extract the maximum of information. It is also remarkably independent of particular astrophysical assumptions, since no use is made of benchmarks events. The basic idea is the following: in the idealized case of vanishing experimental errors in the determination of the neutrino energies and arrival times, and assuming an arbitrarily large statistics and a perfectly blackbody neutrino spectrum, one could use the events with energy above some suitable value E^* (to suppress the mass effects) to reconstruct very precisely the evolution in time of the neutrino flux and spectrum. Once the time dependence of the full signal is pinned down, the only parameter left to reconcile the time distribution of the low energy neutrinos with the high energy part of the signal would be the neutrino mass, which could then be nailed to its true value. Of course, none of the previous conditions is actually fulfilled. In water Cerenkov detectors as SuperKamiokande (SK) the uncertainty on relative timings is negligible; however, the errors in the energy measurements are important and must be properly taken into account. The statistics is large but finite, and this not only represents a source of statistical uncertainty, but also implies an upper limit on the useful values of E^*. Finally, the SN neutrino spectrum is not perfectly thermal [17]. Nevertheless, a good sensitivity to the mass survives and, as we will show, it will be possible to disentangle with a good confidence the two cases $m_\nu = 0$ and 1 eV.

To test quantitatively the idea outlined above we proceed in two steps.

(i) First we generate a set of synthetic neutrino signals, according to some suitable SN model. Neutrinos are then propagated from the SN to the detector assuming two different SN-Earth distances (10 and 20 kpc) and two different mass values $m_\nu = 0$ and 1 eV. Finally, two different energy thresholds (5 and 10 MeV) are used for the detection. The result consists of several neutrino samples that hopefully would not differ too much from a real SN signal.

(ii) The signals are then analyzed with the main goal of disentangling with sufficient confidence the two cases $m_\nu = 0$ and 1 eV. Only the SN-Earth distance is assumed to be known (this information could be obtained directly from optical observations or, with an uncertainty of the order of 25%, from a comparison of the measured total energy with a theoretical estimation of the binding energy released [18]). Other quantities, like the spectral functions and the details of the time evolution of the neutrino flux, are inferred directly from the data.

Generation of the neutrino samples. The time evolution of the neutrino luminosity and average energy can be obtained from the results of SN explosion simulations [19–22]. In the present analysis we use the results of Woosley *et al.* [20]. This model is characterized by a rather hard neutrino spectrum ($\langle E_{\bar{\nu}_e} \rangle \gtrsim 20$ MeV) that results in a large number of detected events (8,800 in SK). Still this is a conservative

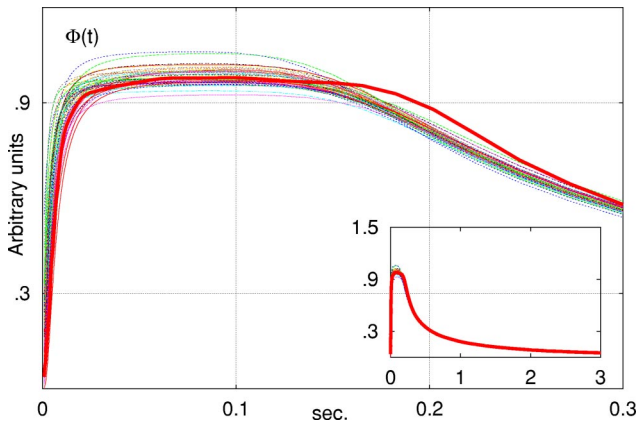

FIG. 2. Comparison between the Monte Carlo flux function $\hat{\Phi}(t)$ (thick line) and the result of the likelihood analysis for 40 samples ($L = 10$ kpc, $E_{tr} = 5$ MeV, $m_\nu = 0$).

choice, since it also implies a depletion in the number of low energy neutrinos with a corresponding loss of information on the neutrino mass. Inside the protoneutron star neutrinos are in thermal equilibrium, and therefore it is reasonable to assume that the gross features of their energy spectrum after emission can still be described by a Fermi-Dirac distribution:

$$\hat{S}(E_\nu; \hat{T}(t), \hat{\eta}) = \frac{E_\nu^2/\hat{T}^3(t)}{F_2(0,\hat{\eta})(1+e^{E_\nu/\hat{T}(t)-\hat{\eta}(t)})}, \tag{2}$$

where $F_2(0,\hat{\eta})$ is defined in Eq. (4) and a ''pinching'' factor $\hat{\eta}(t)$ has been introduced to simulate spectral distortions [17]. From now on, quantities with a hat ($\hat{\eta}, \hat{T}, \ldots$) represent input to the Monte Carlo (MC) simulation, while quantities without a hat will refer to results of data fitting. We define the Fermi functions and generalized Fermi integrals as

$$f_n(x,\eta) = \frac{x^n}{1+e^{x-\eta}} \tag{3}$$

$$F_n(y,\eta) = \int_y^\infty f_n(x,\eta)\ dx. \tag{4}$$

Using the time evolution of the average neutrino energy $\overline{E_\nu}(t)$ as given in Fig. 3 of Ref. [20] and taking for simplicity $\hat{\eta} = 3$ [17] constant, we compute the effective temperature that, together with $\hat{\eta}$, determines the neutrino spectrum at the source:

$$\hat{T}(t) = k_3 \overline{E_\nu}(t), \tag{5}$$

where $k_3 \equiv F_2(0,3)/F_3(0,3) \approx 4$. Given that the average energy is only mildly dependent on time [20], we model the evolution of the neutrino flux $\hat{\Phi}(t)$ simply by taking it proportional to the luminosity as given in Fig. 2 of Ref. [20].

In the SK detector, $\bar{\nu}_e$'s are detected through the inverse β decay reaction $\bar{\nu}_e p \to e^+ n$ that has the energy threshold $E_{\rm react} = m_e + \Delta m_{np} \simeq 1.8$ MeV, where m_e is the electron mass

and $\Delta m_{np} \simeq 1.3$ MeV is the neutron to proton mass difference. The effect of the detection cross section $\sigma(E_\nu)$ [23] is taken into account from the beginning by using the function $\hat{S}(E_\nu;\hat{T}(t),\hat{\eta})\times\hat{\Phi}(t)\times\sigma(E_\nu)$ in the MC generator. Each SN neutrino is labeled by its emission time t_ν and by its energy E_ν. The corresponding detected positron is also identified by an energy/time pair of values (E^e,t^e). We generate E^e according to a Gaussian distribution with central value $E^e = E_\nu - \Delta m_{np}$ and variance $\sigma = 0.15\sqrt{10\text{MeV}/E^e}$ that corresponds to the SK energy resolution [24]. Since the time resolution of the SK detector is very precise, no error is assigned to t^e. For massive neutrinos, we redefine $t^e = t_\nu + \Delta t_\nu$ by including the appropriate delay $\Delta t_\nu = L m_\nu^2/2E_\nu^2$. A fixed number of 8,800 energy/time pairs (E_i^e,t_i^e) is generated in each run. This corresponds to the expected number of $\overline{\nu_e}$ interactions within the SK fiducial volume for the spectrum of the model in [20] and a SN at 10 kpc. For $L=20$ kpc this number is resampled down by a factor of four. Next, positrons with energies below the detection threshold ($E_{\text{tr}}=5$ or 10 Mev) are discarded, and as a last step the origin of the time axis is set in coincidence with the first positron detected ($t_1^e=0$) and each t_i^e is accordingly redefined. For each set of values (E_{tr},L,m_ν) 40 different samples are generated in this way.

Analysis of the neutrino signal. We analyze the neutrino signals by means of the likelihood function

$$\mathcal{L} = S(\epsilon;T(t),\eta(t))\times\Phi(t+\delta t;b,d,f)\times\sigma(\epsilon). \tag{6}$$

The energy $\epsilon = E^e + \Delta m_{np}$ of each neutrino is inferred from the positron energy. The spectral function S is assumed of the form (2) with a time-dependent effective temperature $T(t)$ and pinching factor $\eta(t)$ fitted from the data. $\Phi(t+\delta t;b,d,f)$ describes the time evolution of the neutrino flux, and the four parameters δt, b, d and f account for its location on the time axis and detailed shape. Finally, $\sigma(\epsilon)$ is the neutrino cross section.

The spectral functions. The two spectral functions $T(t)$ and $\eta(t)$ are determined by fitting the first and second momentum of the energy distribution to the mean energy $\overline{E_\nu}$ and mean squared energy $\overline{E_\nu^2}$ of the *incoming* neutrino flux (prior to detection). Given a set of n neutrinos with *measured* energies $(\epsilon_1,\epsilon_2,\ldots,\epsilon_n)$, and assuming for the cross section the approximate form $\sigma(\epsilon)\propto\epsilon^2$, we have

$$\overline{E_\nu} \approx \frac{\sum_i \epsilon_i^{-1}}{\sum_i \epsilon_i^{-2}}, \quad \overline{E_\nu^2} \approx \frac{n}{\sum_i \epsilon_i^{-2}}. \tag{7}$$

From Eq. (1) we see that the typical neutrino delays are at most of the order of few milliseconds. This is much shorter than the time scale over which sizable variations of the spectral functions are likely to occur [19–22]. Therefore, by binning over sufficiently large time windows we can ensure that the determination of T and η for each bin will not be affected by the delays. We use a set of 20 windows of size increasing from 50 ms to 2 s, distributed over a signal duration 20 s. After this time the neutrino flux is assumed to be too low to provide additional information. To reduce further the possible effects of mass-induced time delays, only neutrinos with energy larger than $E^*=15$ MeV are used. For each time window $[t_a,t_{a+1}]$ we perform a least square fit to the following quantities:

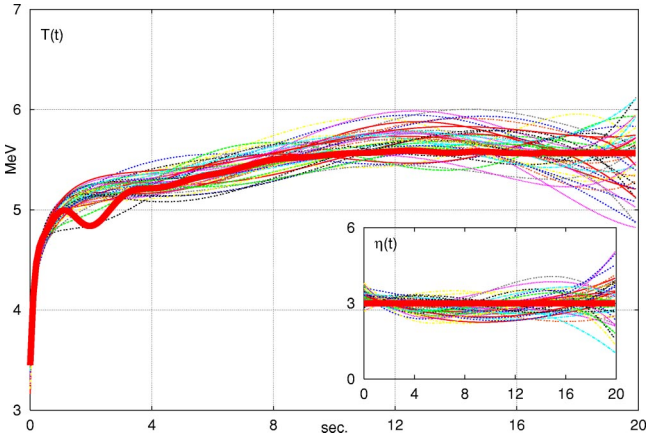

FIG. 1. Comparison of the Monte Carlo spectral temperature $\hat{T}(t)$ and pinching parameter $\hat{\eta}$ (thick lines) with $T(t)$ and $\eta(t)$ fitted for 40 samples ($L=10$ kpc, $m_\nu=0$).

$$\overline{E_\nu}(T,\eta) = \frac{F_3(y,\eta)}{F_2(y,\eta)}T, \tag{8}$$

$$\frac{\overline{E_\nu^2}(T,\eta)}{[\overline{E_\nu}(T,\eta)]^2} = \frac{F_2(y,\eta)F_4(y,\eta)}{F_3^2(y,\eta)}, \tag{9}$$

where the functions $F_n(y,\eta)$ defined in Eq. (4) depend on the temperature through $y=E^*/T$. This yields the "best" values $T(\overline{t_a})$ and $\eta(\overline{t_a})$ at $\overline{t_a}=(t_a+t_{a+1})/2$. Finally, in order to obtain two smooth continuous functions, the points $T(\overline{t_a})$ and $\eta(\overline{t_a})$ are interpolated with two half integer power polynomials $P_{T,\eta}\sim\Sigma_l c_l t^{l/2}$ with $l=0,1,2,\ldots 10$ for T and $l=0,1,3,5$ for η. In Fig. 1 the functions $\hat{T}(t)$ and $\hat{\eta}=3$ used in the simulation MC simulation (thick lines) are compared with 40 fits to neutrino samples generated with $m_\nu=0$ and $L=10$ kpc. These results remain unchanged for $m_\nu=1$ eV, while for $L=20$ kpc, due to the reduced statistics, the fits show a somewhat wider dispersion.

The neutrino flux. Even if the details of the neutrino flux evolution with time are not known, its gross features can be predicted on rather solid theoretical grounds. It is expected that a sharp exponential rise, with a time scale of tenths of milliseconds, is followed by a power law decay, with a time scale of several seconds. We model this behavior by means of a parametric analytical function in which, roughly speaking, two parameters describe the rising and decaying rates, and a third one accounts for the transition point:

$$\Phi(t;b,d,f) \sim \frac{e^{-ft^{-m}}}{(1+bt^n)^d} \to \begin{cases} e^{-ft^{-m}} & (t\to 0) \\ t^{-nd} & (t\to\infty). \end{cases} \tag{10}$$

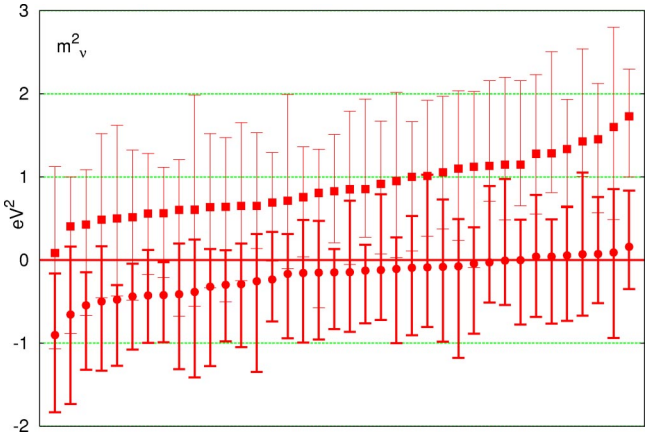

FIG. 3. Fitted values of the mass and 95% C.L. error bars for two sets of 40 analysis with $L=10$ kpc and $E_{tr}=5$ MeV for $\hat{m}_\nu=0$ (circles) and $\hat{m}_\nu=1$ eV (squares).

This function can reproduce reasonably well the results of different models [19–22]. The two exponents m and n are fixed to suitable integer values by means of a preliminary rough fitting procedure to the data, and then are held constant throughout the analysis of all the samples. For the model in [20] we use $n=8$ and $m=2$. Finally, since the origin of times was arbitrarily set in coincidence with the detection of the first neutrino while Φ vanishes at $t=0$, a fourth parameter δt is required to let $\Phi(t+\delta t)$ freely shift along the time axis.

The likelihood analysis. The minimization of the negative log-likelihood is carried out by means of the package MINUIT [25]. To avoid double minimums, we minimize with respect to the square of the neutrino mass. Given a value of m_ν^2 the time delay of each neutrino is computed according to its energy ϵ_i, and subtracted from its arrival time t_i. The log-likelihood for the new array of times is then evaluated, and minimized with respect to the other parameters b, d, f and δt. This proceeds until the absolute minimum is found in the full five-dimensional parameter space. There is a subtlety related to the cases when, especially for large test masses, a neutrino is migrated to an early time where $\Phi=0$. The problem is not just a numerical one of logarithm overflow. Due to the uncertainty in the energy measurement, the first neutrinos detected can end up in such a position without necessarily implying that the corresponding distribution has vanishing probability. To account for this, for the relevant neutrinos the energy uncertainty is converted into an uncertainty in the new time position, and the corresponding contribution to the likelihood is evaluated by convolving $\mathcal{L}(t)$ in Eq. (10) with a Gaussian of the appropriated width. In Fig. 2 the results of the fitted fluxes for 40 samples with $L=10$ kpc, $E_{\rm tr}=5$ MeV and $m_\nu=0$ eV are compared with the function $\hat{\Phi}(t)$ used in the MC generator (thick line).

Results. Our results are summarized in Fig. 3 and in Table I. Figure 3 depicts the results of the mass fits for two sets of 40 samples with $E_{\rm tr}=5$ MeV, $L=10$ kpc, $\hat{m}_\nu=0$ (circles) and $\hat{m}_\nu=1$ eV (squares). The data points have been ordered with an increasing value of the best fit mass to show the difference between the two cases. Error bars correspond to 95% C.L., where the lower (upper) limit is computed by integrating the likelihood from $m_\nu^2=\infty$ $(-\infty)$ until reaching the 95% of the area, while minimizing with respect to the other parameters. We have checked that the limits do not change much if the integration is restricted to the physical region $m_\nu^2>0$.

TABLE I. Results of the analysis for the two neutrino masses $\hat{m}_\nu=0$ and 1 eV, two energy thresholds of 5 and 10 MeV and for two SN distances of 10 kpc and, in parentheses, 20 kpc. The first (second) row give the percentage of times in which the 95% C.L. lower (upper) limit m_ν^l (m_ν^u) is larger (smaller) than $\hat{m}_\nu$. The third row lists how many times $m_\nu=0$ can be excluded (95% C.L.) when $\hat{m}_\nu=1$ eV. The following three rows give, for $L=10$ kpc, the mass square best fit and the 95% lower and upper limits averaged over 40 samples.

$E_{\rm tr}$	5 MeV		10 MeV	
$\hat{m}_\nu$ (eV)	0	1	0	1
$m_\nu^l>\hat{m}_\nu$(%)	5 (11)	4 (5)	5 (10)	11 (5)
$m_\nu^u<\hat{m}_\nu$(%)	9 (6)	2 (5)	12 (6)	10 (7)
$m_\nu^l>0$(%)	–	55 (40)	–	28 (23)
$\langle m_\nu^2\rangle$	-0.1 ± 0.4	1.0 ± 0.5	-0.2 ± 0.8	0.8 ± 1.0
$\langle(m_\nu^l)^2\rangle$	-0.8 ± 0.4	0.1 ± 0.6	-1.6 ± 1.0	-0.8 ± 1.2
$\langle(m_\nu^u)^2\rangle$	0.6 ± 0.5	1.8 ± 0.5	1.1 ± 1.0	2.2 ± 1.1

Table I summarizes some results of the mass fitting. For each set of parameters $(E_{\rm tr},L,\hat{m}_\nu)$ we have analyzed 40 samples. The first row gives the percentage of times in which the 95% C.L. lower limit m_ν^l is *larger* than the input mass $\hat{m}_\nu$. The second row refers to the cases when the upper limit m_ν^u is *smaller* than $\hat{m}_\nu$. The numbers in parentheses correspond to $L=20$ kpc. These figures characterize the percentage of ''failures'' of the method, which therefore appear to be reliable in about 90–95 % of the cases. The third row gives the percentage of times when $m_\nu=0$ is excluded at 95% C.L. when the signal is generated with $\hat{m}_\nu=1$ eV. This characterizes the power of the method for excluding a massless neutrino. We see that in the most favorable case ($E_{\rm tr}=5$ MeV, $L=10$ kpc) the method is successful in more than 50% of the cases. The following three rows give the average over the 40 samples of the mass square best fit and of the 95% C.L. lower and upper limits (only for $L=10$ kpc). These last figures are just intended to give an idea of the quality of the fits (they would be fully meaningful only if 40 SN could be observed).

From the results in the table it is apparent that low energy neutrinos are crucial for the sensitivity of the method, and therefore a low detection threshold is very important. With $E_{\rm tr}=5$ MeV the massless case is excluded in about 50% of the cases, while this drops to 25% when $E_{\rm tr}=10$ MeV. Also, with the higher energy threshold the fluctuations of the results over the 40 runs is doubled (last three rows). Unfortunately, there could be a dangerous background in the energy range between 5 and 10 MeV, represented by photons originating from neutral current reactions off ^{16}O mainly pro-

duced by the more energetic μ and τ neutrinos [26]. Softer neutrino spectra, such as the spectra predicted by the model of Totani et al. [21], would have the double benefit of drastically reducing this background, while at the same time raising the number of $\bar{\nu}_e$ emitted in the 5–10 MeV energy range from about 7% of the present analysis to about 20%. In this case a better sensitivity to the mass could be expected. We should also mention that very recently it has been suggested that water Čerenkov detectors could be modified to allow tagging of the inverse β decay neutrons [27]. This would eliminate the background from neutral current reactions and allow for lower thresholds.

Numerical spectrum and neutrino oscillations. The previous results have been derived by relying on two main simplifying approximations for the neutrinos energy spectrum: (1) the neutrino energies have been generated assuming the ''pinched'' Fermi-Dirac spectrum given in Eq. (2) and fitted, as was described above, with a similar two-parameters energy distribution; (2) no effects of the neutrino oscillations were included in the analysis. In order to evaluate to what extent the sensitivity of the method could be affected by these approximations, we have run a set of simulations in which the neutrino energies were generated according to the shapes of the numerical spectra given by Janka and Hillebrandt in [17]. A time-dependent energy rescaling of the spectral shapes was introduced to reproduce properly the time evolution of the mean energies as given in [20]. We stress that since a two parameter Fermi-Dirac distribution fits rather accurately the spectra obtained from the numerical simulations, dropping our first simplification does not affect sensibly the numerical results.

Neutrino oscillations can produce a composite spectrum corresponding to an admixture of the original $\bar{\nu}_e$ spectrum with a harder component due to $\bar{\nu}_x$ $(x=\mu,\tau)$ [28]. Clearly, the resulting spectral distortions will depend on the size of the $\bar{\nu}_e-\bar{\nu}_x$ spectral differences. While it is often stated that these differences could be quite sizable, and could yield up to a factor of two hierarchy between the $\bar{\nu}_x$ and $\bar{\nu}_e$ average energies [19–22], recent and more complete analyses of SN neutrino spectra formation [29] indicate that this is not the case: the inclusion of important interaction rates that were neglected in previous works yields spectral differences that are only of the order of 10% [29]. At this level, identifying the two components of a mixed spectrum would be a difficult task, and could represent a real challenge for the study of SN neutrino oscillations in the $\bar{\nu}_e-\bar{\nu}_x$ channel. However, for what concerns our analysis, this ensures that the results discussed above are not affected much by neutrino oscillations. To be on the safe side, we have tested the sensitivity of our method to oscillation effects by running a set of simulations using the results of Woosley *et al.* [20] for which, as a consequence of neglecting important neutrino reactions [29], the spectral differences are extreme ($\bar{E}_{\bar{\nu}_x}\approx 2\bar{E}_{\bar{\nu}_e}$). As we will show, even in this (probably unrealistic) case, we find that the loss in sensitivity to the neutrino mass is small. We can conclude that the effects of neutrino oscillations do not endanger the applicability of our method and neither its overall sensitivity to the neutrino mass.

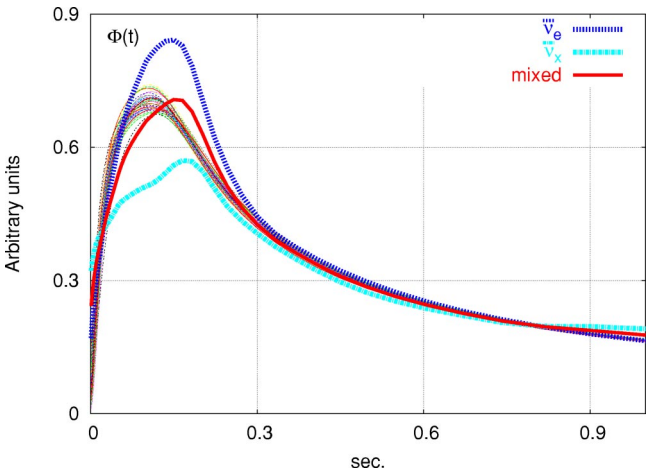

FIG. 4. Comparison between the $\bar{\nu}_e$ (upper thick line) and $\bar{\nu}_\mu$ (lower thick line) fluxes used in the Monte Carlo, the resulting $\bar{\nu}_e$ flux at the detection point (middle thick line), and the maximum likelihood fits for 40 neutrino samples with a mixed composite spectrum.

As is discussed in [28], depending on the type of the neutrino mass hierarchy (normal or inverted) and on the size of $\sin^2\theta_{13}$ (large $\gtrsim 10^{-4}$ or very small $\lesssim 10^{-6}$), neutrino oscillations could (i) harden the $\bar{\nu}_e$ spectrum through a complete spectral swap with $\bar{\nu}_\mu$ (inverted hierarchy, large θ_{13}), (ii) mix the $\bar{\nu}_e$ spectrum with a fraction of about $\sin^2\theta_{12}\sim 1/4$ of harder neutrinos (in the other cases). (The region $\sin^2\theta_{13}\sim 10^{-6}$–$10^{-4}$ would produce spectra with an intermediate amount of mixing.) The first case can be studied without modifications in our procedure. Clearly, a different spectrum would imply somewhat different numerical results; however, this is analogous to the unavoidable uncertainty related to the choice of the particular SN model since, for example, the $\bar{\nu}_e$ mean energies that have been used in the present analysis [20] are quite close to the $\bar{\nu}_\mu$ mean energies of the model of Totani *et al.* [21]. The second case is more interesting since, for large spectral differences, fitting a composite spectrum with just one effective spectral temperature and one pinching parameter could degrade somewhat the sensitivity.

We have carried out an analysis of 40 neutrino samples with a mixed composite spectrum as would result from a normal mass hierarchy, $\sin^2\theta_{12}\approx 1/4$ and large θ_{13}. The original $\bar{\nu}_e$ and $\bar{\nu}_x$ fluxes taken from [20] are depicted in Fig. 4 and compared with the composite $\bar{\nu}_e$ flux at the detection point, as well as with our maximum likelihood fits. The relative normalization of the fluxes was computed assuming flavor equipartition of the integrated luminosities and the time-dependent average energies given in [20]. A similar comparison between the mean energies of the two spectral components, the average energy of the mixed spectrum and the average energies obtained from Fermi-Dirac distributions with fitted spectral parameters $\hat{T}(t)$ and $\hat{\eta}(t)$ is depicted in Fig. 5.

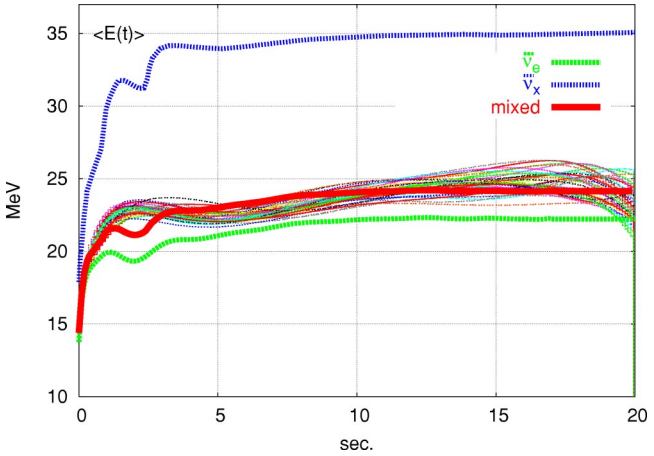

FIG. 5. Comparison between the $\overline{\nu}_e$ (lower thick line) and $\overline{\nu}_\mu$ (upper thick line) mean energies of the numerical spectra used in the Monte Carlo, the mean energy of the mixed composite spectrum (middle thick line), and the fitted values of $\overline{E}_{\overline{\nu}_e}(t)$ for 40 neutrino samples.

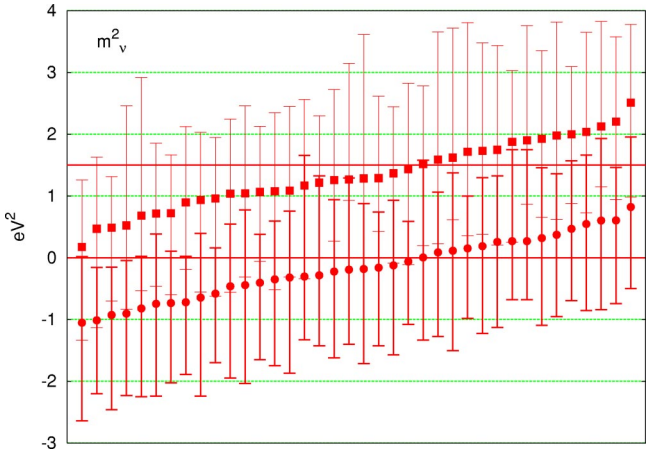

FIG. 6. Fitted values of the mass and 95% C.L. error bars for a set of 40 neutrino samples with mixed composite spectra ($L=10$ kpc, $E_{tr}=5$ MeV, $\hat{m}_\nu=0$ (circles), $\hat{m}_\nu=1.2$ eV (squares)).

For the mass fits we have taken $E_{\rm tr}=5$ MeV and $L=10$ kpc. Since we are essentially interested in the loss of sensitivity to the neutrino mass with respect to the non-oscillation case, we have been searching for a mass value that can reproduce results similar to those of the band plot in Fig. 3 (namely, for a signal generated with $\hat{m}_\nu\neq 0$ we require the massless case to be excluded at 95% C.L. in at least 50% of the runs). As is shown in Fig. 6 our requirement is fullfilled for $\hat{m}_\nu=1.2$ eV, to be compared with $\hat{m}_\nu=1.0$ eV for the non-oscillation case. We conclude that even in the unrealistic case of extremely large spectral differences between the components of a mixed spectrum, fitting the data with a single two parameter Fermi-Dirac distribution does not degrade much the numerical results for the mass estimate. Given that the most recent results suggest that the $\overline{\nu}_e$ and $\overline{\nu}_\mu$ spectra are in fact not very different [29], the use of more complicated bimodal energy distributions to improve the mass fits is probably not justified.

Before concluding, a few remarks are in order. In this work we have not carried out any deep study aimed to optimize the single fits to each different neutrino sample (windows size, interpolating functions $P_{T,\eta}$, specific flux function parameters). A large number of different sets of data have been analyzed through the very same procedure, in order to collect enough information about the sensitivity of the method in a reasonable amount of time. It is clear to us that optimizing the overall procedure in order to analyze a specific sample (as would certainly be the case with a signal from a real SN) can improve the sensitivity and shrink somewhat the uncertainties on m^2_ν.

Besides the effects of neutrino oscillations that were briefly analyzed in the last paragraph, a few other issues deserve further investigation. For example, assuming that the SK signal could be combined with negligible uncertainty on the absolute timing with the signal detected at KamLAND, the much better energy resolution and the lower threshold of this last detector could enhance the sensitivity to the neutrino mass. It also remains to see what sensitivity could be achieved with a statistics one order of magnitude larger, as would be available with the megaton neutrino detectors presently under study [30–32].

We acknowledge conversations with H.-T. Janka, G. Raffelt and in particular with A. Yu. Smirnov. J.I.Z. acknowledges hospitality from the Abdus Salam ICTP in Trieste (Italy) during the final stage of this research, and Colciencias for financial support. This work was supported in part by Colciencias in Colombia under contract 1115-05-13809.

[1] S. Fukuda *et al.*, Phys. Rev. Lett. **86**, 5651 (2001); Q. Ahmad *et al.*, *ibid.* **87**, 071301 (2001).
[2] Y. Fukuda *et al.*, Phys. Rev. Lett. **81**, 1562 (1998); **82**, 2644 (1999); M. Ambrosio *et al.*, Phys. Lett. B **434**, 451 (1998); **478**, 5 (2000).
[3] K. Eguchi *et al.*, Phys. Rev. Lett. **90**, 021802 (2003).
[4] H. Pas and T.J. Weiler, Phys. Rev. D **63**, 113015 (2001); S. Bilenky *et al.*, Phys. Rep. **379**, 69 (2003).
[5] J. Bonn *et al.*, Prog. Part. Nucl. Phys. **48**, 133 (2002); V.M. Lobashev *et al.*, Nucl. Phys. B (Proc. Suppl.) **91**, 280 (2001).
[6] H.V. Klapdor-Kleingrothaus *et al.*, Eur. Phys. J. A **12**, 147 (2001); C.E. Aalseth *et al.*, Phys. Rev. D **65**, 092007 (2002).
[7] D.N. Spergel *et al.*, Astrophys. J., Suppl. Ser. **148**, 175 (2003).
[8] M. Colless *et al.*, Mon. Not. R. Astron. Soc. **328**, 1039 (2001).
[9] S. Hannestad, J. Cosmol. Astropart. Phys. **0305**, 004 (2003); O. Elgaroy and O. Lahav, *ibid.* **0304**, 004 (2003).
[10] G.T. Zatsepin, Zh. Éksp. Teor. Fiz. **8**, 333 (1968) [JETP Lett. **8**, 205 (1968)]; S. Pakvasa and K. Tennakone, Phys. Rev. Lett. **28**, 1415 (1972).
[11] D.N. Schramm, Comments Nucl. Part. Phys. **17**, 239 (1987).
[12] T.J. Loredo and D.Q. Lamb, Phys. Rev. D **65**, 063002 (2002).
[13] D. Fargion, Lett. Nuovo Cimento Soc. Ital. Fis. **31**, 499 (1981).

[14] N. Arnaud *et al.*, Phys. Rev. D **65**, 033010 (2002).
[15] T. Totani, Phys. Rev. Lett. **80**, 2039 (1998).
[16] J.F. Beacom, R.N. Boyd, and A. Mezzacappa, Phys. Rev. Lett. **85**, 3568 (2000); Phys. Rev. D **63**, 073011 (2001).
[17] H.-T. Janka and W. Hillebrandt, Astron. Astrophys. **224**, 49 (1989).
[18] J.F. Beacom and P. Vogel, Phys. Rev. D **60**, 033007 (1999).
[19] A. Burrows, D. Klein, and R. Gandhi, Phys. Rev. D **45**, 3361 (1992).
[20] S.E. Woosley *et al.*, Astrophys. J. **433**, 229 (1994).
[21] T. Totani *et al.*, Astrophys. J. **496**, 216 (1998).
[22] M. Liebendorfer *et al.*, Phys. Rev. D **63**, 103004 (2001).
[23] A. Strumia and F. Vissani, Phys. Lett. B **564**, 42 (2003).
[24] M. Nakahata *et al.*, Nucl. Instrum. Methods Phys. Res. A **421**, 113 (1999).
[25] F. James and M. Roos, Comput. Phys. Commun. **10**, 343 (1975).
[26] K. Langanke, P. Vogel, and E. Kolbe, Phys. Rev. Lett. **76**, 2629 (1996).
[27] J.F. Beacom and M.R. Vagins, hep-ph/0309300.
[28] See, e.g., C. Lunardini and A.Y. Smirnov, J. Cosmol. Astropart. Phys. **0306**, 009 (2003), and references therein.
[29] M.T. Keil, G.G. Raffelt, and H.T. Janka, Astrophys. J. **590**, 971 (2003); G.G. Raffelt, M.T. Keil, R. Buras, H.T. Janka, and M. Rampp, astro-ph/0303226; M.T. Keil, astro-ph/0308228.
[30] K. Nakamura, talk given at the conference ''Neutrinos and Implications for Physics Beyond the Standard Model,'' Stony Brook, NY, 2002 [www.physics.sunysb.edu/itp/conf/ neutrino/ talks/nakamura.pdf]
[31] C.K. Jung, hep-ex/0005046.
[32] Y. Suzuki *et al.*, Proceedings of the 2nd International Workshop ''Neutrino Oscillations and their Origin (NOON 2000),'' Tokyo, 2000 (World Scientific, Singapore, 2001), pp. 288–298, hep-ex/0110005.